

# TNF- $\alpha$ plays a role in hepatocyte apoptosis in Niemann-Pick type C liver disease

Victoria M. Rimkunas,\* Mark J. Graham,<sup>†</sup> Rosanne M. Crooke,<sup>†</sup> and Laura Liscum<sup>1,\*</sup>

Department of Physiology,\* Tufts University School of Medicine, 136 Harrison Avenue, Boston, MA 02111; and Cardiovascular Disease Antisense Drug Discovery,<sup>†</sup> Isis Pharmaceuticals, Inc., 1896 Rutherford Road, Carlsbad, CA 92008

**Abstract** Niemann-Pick type C (NPC) is a fatal autosomal recessive lysosomal storage disease clinically characterized by neurodegeneration and liver disease. Heterogeneous mutations in the *NPC1* and *NPC2* genes cause impaired egress of free cholesterol from lysosomes, leading to accumulation of cholesterol and glycosphingolipids. Key features of NPC liver disease include hepatic apoptosis, inflammation, and fibrosis. It is unclear what signaling events regulate these disease processes in NPC. We hypothesize that tumor necrosis factor  $\alpha$  (TNF- $\alpha$ ), which is involved in both proinflammatory and apoptotic signaling cascades, is a key mediator of inflammation, apoptosis, and fibrosis in NPC liver disease. **In this study, we evaluated the role of TNF- $\alpha$  signaling in NPC liver disease by utilizing NPC1-specific antisense oligonucleotides to knock down NPC1 expression in control and TNF- $\alpha$  knockout mice. In the absence of TNF- $\alpha$ , NPC1 knockdown produced liver disease with significantly less inflammation, apoptosis, and fibrosis.**—Rimkunas, V. M., M. J. Graham, R. M. Crooke, and L. Liscum. **TNF- $\alpha$  plays a role in hepatocyte apoptosis in Niemann-Pick type C liver disease.** *J. Lipid Res.* 2009. 50: 327–333.

**Supplementary key words** cholesterol • sphingosine • macrophage • fibrosis • inflammation

Niemann-Pick type C (NPC) disease is a fatal neurodegenerative disease characterized by lysosomal storage of cholesterol and glycosphingolipids in every cell of the body. Mutations in the *NPC1* gene are responsible for approximately 95% of human NPC disease (1). The majority of NPC patients die due to neurodegenerative complications; however, the liver disease is also significant (2).

NPC disease is the second most common cause of neonatal cholestasis (3). Multiple cases have reported patients suffering from liver failure (3–9). Ten percent of NPC infants presenting with neonatal cholestasis die from liver failure before they reach 6 months of age (10). Patients

who do not die as infants often live with persistent liver disease accompanied by fibrosis and, in rare cases, cirrhosis. The cause of NPC liver disease is unknown. Recent studies in NPC-deficient mice suggest that hepatocyte apoptosis may be a primary cause of liver dysfunction and liver failure (11, 12).

The inflammatory cytokine tumor necrosis factor  $\alpha$  (TNF- $\alpha$ ) has been implicated in NPC disease progression. Multiple members of the TNF- $\alpha$  pathway are overexpressed in NPC liver and brain (11–13). TNF- $\alpha$  plays a very important role in apoptosis of hepatocytes as well as their regeneration (14, 15). TNF- $\alpha$  that is secreted by foamy macrophages recruits inflammatory cells, stimulates hepatic stellate cells, which deposit collagen, and signals apoptosis of hepatocytes (16–20). The multifunctional roles of TNF- $\alpha$  identify it as a potential key regulator of several aspects of NPC liver disease. For these reasons, the goal of our study was to determine whether TNF- $\alpha$  plays a role in the pathogenesis of NPC liver disease.

In our previous work, we developed a novel mouse model for liver-specific knockdown of NPC1 protein expression in vivo by administration of antisense oligonucleotides (ASOs) (12). For this study, we reduced NPC1 expression in TNF- $\alpha$ -deficient mice in order to assess the role of TNF- $\alpha$  in NPC liver disease. We conclude that in the absence of TNF- $\alpha$ , the progression of NPC liver disease is slowed, such that hepatocyte apoptosis, fibrosis, and foamy macrophage clustering are attenuated.

## EXPERIMENTAL PROCEDURES

### Oligonucleotides

The 20 mer 2'-O-methoxyethyl-modified ASOs were synthesized and purified as described previously (21, 22). The sequence

*This work was supported by National Institutes of Health Grants R01 DK-49564 and T32 DK-07542 and a predoctoral fellowship from the American Heart Association (0615665T).*

*Manuscript received 5 August 2008 and in revised form 17 September 2008.*

*Published, JLR Papers in Press, September 24, 2008.  
DOI 10.1194/jlr.M800415-JLR200*

Abbreviations: ALT, alanine aminotransferase; ASO, antisense oligonucleotide; AST, aspartate aminotransferase; BrdU, bromodeoxyuridine; NPC, Niemann-Pick type C disease; TNF- $\alpha$ , tumor necrosis factor  $\alpha$ ;  $\alpha$ -sma,  $\alpha$  smooth muscle actin.

<sup>1</sup>To whom correspondence should be addressed.  
e-mail: laura.liscum@tufts.edu

of the ASO targeted to the NPC1 mRNA is 5'CCCGATTGAGCTCATCTTCG3'. As a control, we used an ASO with a mismatched sequence 5'CCTTCCCTGAAGGTTCTCC3'. ASOs were dissolved in 0.9% saline and stored at  $-20^{\circ}\text{C}$ .

### Animal care and treatment

All of the following procedures were approved by the Institutional Animal Care and Use Committee at Tufts University and were in compliance with the National Institutes of Health Guide for the Care and Use of Laboratory Animals. Female C57BL/6 and 129S6-Tnf<sup>tm1Gkl/J</sup> mice (6–8 weeks of age) were purchased from The Jackson Laboratory (Bar Harbor, ME). They were housed five animals per cage and fed rodent chow. Mice were injected intraperitoneally with either NPC1 ASO or a mismatched control ASO at a dose of 100 mg/kg/week for 9 weeks. At the end of the treatment period, animals were fasted overnight, then euthanized, and blood samples were taken by cardiac puncture. Mice were perfused with cold PBS via cardiac puncture, after which, tissues were dissected and fixed in 10% formalin or snap-frozen.

### Western blots

Liver tissue was blotted for NPC1 as previously described (12) using an NPC1 antibody from Abcam (Cambridge, MA). Anti- $\alpha$ -gapdh monoclonal antibody was purchased from BioRad Laboratories (Hercules, CA) and used at 1:1,000 dilution.

### Measurement of cholesterol and sphingosine content

Aliquots of 100  $\mu\text{g}$  liver homogenate were subjected to extraction according to the method of Folch, Lees, and Sloane Stanley (23). Stigmasterol (15  $\mu\text{g}$ ) was added to each sample as an internal standard. The Folch organic phase was then used for unesterified cholesterol measurements quantified by a Hewlett-Packard 5890 gas chromatograph using a DB-17 capillary column (15 m  $\times$  0.53 mm; Alltech) at  $255^{\circ}\text{C}$ . Sphingosine was analyzed from 2 mg aliquots of liver homogenate by HPLC and liquid chromatography-MS by the Lipidomic Core Mass Spectrometry Lab at Medical University of South Carolina as previously described (24).

### Serum chemistries

Blood was centrifuged at 2,000 *g* for 15 min, and aspartate aminotransferase (AST) and alanine aminotransferase (ALT) were measured by Idexx Laboratories (Grafton, MA).

### Histology

Liver tissue was fixed in 10% formalin and paraffin embedded. Four micron sections were stained with Masson Trichrome, hematoxylin-eosin, or anti- $\alpha$  smooth muscle actin ( $\alpha$ -sma) by the Tufts Animal Histology Core and Tufts Medical Center Histology Department. The number of lipid-laden and  $\alpha$ -sma-positive cells were quantified by counting the number of positive cells per field at 200 $\times$  magnification (500 cells per field). The area of clustered macrophages was measured using ImageJ. Collagen deposition was measured by first replacing the blue Masson trichrome stain with pure green in Corel Paint Shop Pro X software. We then analyzed the percentage of green pixels out of the total number of pixels for each image, utilizing the program QuantiColor, designed by Z. Rimkunas. For all tests, five random fields were examined per liver; five animals were evaluated per treatment group.

### Detection of apoptotic and proliferating cells

Apoptotic and proliferating cells in formalin-fixed, paraffin-embedded liver tissue sections were detected using the DeadEnd Fluorometric TUNEL System (Promega, Madison, WI) and the BrdU In-Situ Detection Kit (BD Pharmingen, San Diego, CA),

respectively. Procedures were carried out according to the manufacturers' protocols. For proliferating cells, animals were injected with bromodeoxyuridine (BrdU; 50 mg/kg) intraperitoneally 2 h prior to euthanization. The percentage of apoptotic cells was determined by counting the number of positively stained cells per 15 random 200 $\times$  fields (500 cells per field) per treatment group. Proliferating cells were calculated using the QuantiColor analysis described above.

### Statistical analysis

All values are expressed as means  $\pm$  SD. Statistical analysis was performed by one-way ANOVA followed by Tukey's honestly significant differences test using the Vassar Stats website.

## RESULTS

### Knockout of TNF- $\alpha$ does not alleviate hepatomegaly or lipid storage

Our experimental protocol had four treatment groups: control (C57BL/6) and TNF- $\alpha$  knockout mice (TNF KO), injected with either NPC1 ASOs or mismatched control ASOs. NPC1 protein levels in the liver were completely ablated by NPC1 ASO treatment of C57BL/6 and TNF KO mice (Fig. 1A). The body weights of mice in the four treatment groups were the same (Fig. 1B); however, NPC1 knockdown led to increases in relative liver weight in both C56BL/6 and TNF KO mice (Fig. 1C). As expected, knockdown of NPC1 in C56BL/6 mice led to hepatic accumulation of unesterified cholesterol and sphingosine. The same lipid storage was seen when NPC1 was knocked down in TNF KO mice (Table 1).

Serum liver enzymes were measured in the four treatment groups to determine whether the lack of TNF- $\alpha$  resulted in decreased liver injury. Serum levels of ALT (Fig. 2A) and AST (Fig. 2B) were increased equally when NPC1 was knocked down in C57BL/6 and TNF KO mice. This result indicates that liver injury occurs in the absence of TNF- $\alpha$ . This could be due to the cholesterol accumulation that still remains in NPC1 ASO-treated TNF KO mice. Previous studies have indicated that the amount of lysosomal unesterified cholesterol correlates with liver injury in murine NPC disease (25). Taken together, these data indicate that TNF- $\alpha$  does not play a role in the development of the primary storage phenotype of NPC.

### Knockout of TNF- $\alpha$ alters macrophage clustering and decreases inflammation

Previously, we showed that knockdown of NPC1 led to a 10-fold increase in the number of foamy and vacuolated macrophages, which were organized into large lipid granulomas (12). Here we found that C57BL/6 and TNF KO mice treated with mismatched ASO had scattered foamy macrophages, which represented approximately 1% of the cells (Fig. 3A). NPC1 knockdown in C57BL/6 mice led to an increase in the number of macrophages to 20% of the cell population and their clustering into lipogranulomas, as seen previously. Knockdown of NPC1 in TNF KO mice led to the formation of the identical number of foamy macrophages (Fig. 3A); however, the macrophages had an

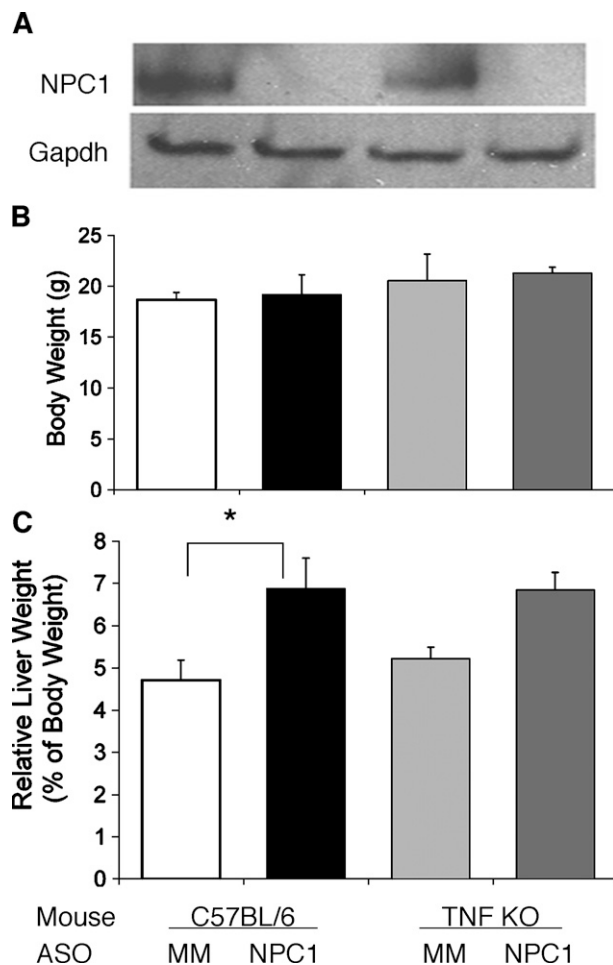


**Fig. 1.** The effect of NPC1 knockdown on whole-body and liver weights. A: Expression of NPC1 in mismatched (MM) and NPC1 antisense oligonucleotide (ASO)-treated control (C57BL/6) and TNF knockout (TNF KO) mice. Immunoblot of GAPDH was used as an internal control. Absolute body (B) and relative liver (C) weights are shown for C57BL/6 and TNF KO mice treated with mismatched (MM) and NPC1 ASOs. Relative liver weight (C) is presented as a percentage of whole-body weight. Each bar represents the mean  $\pm$  SD of 8–19 animals in each treatment group. \* $P < 0.05$ .

altered distribution. They were not gathered in large granulomas but were instead in small clusters (seen in Fig. 4 and quantified in Fig. 3B). The lack of TNF- $\alpha$  may disable macrophage recruitment to sites of hepatocellular injury. NPC1 knockdown in C57BL/6 led to significant recruitment of

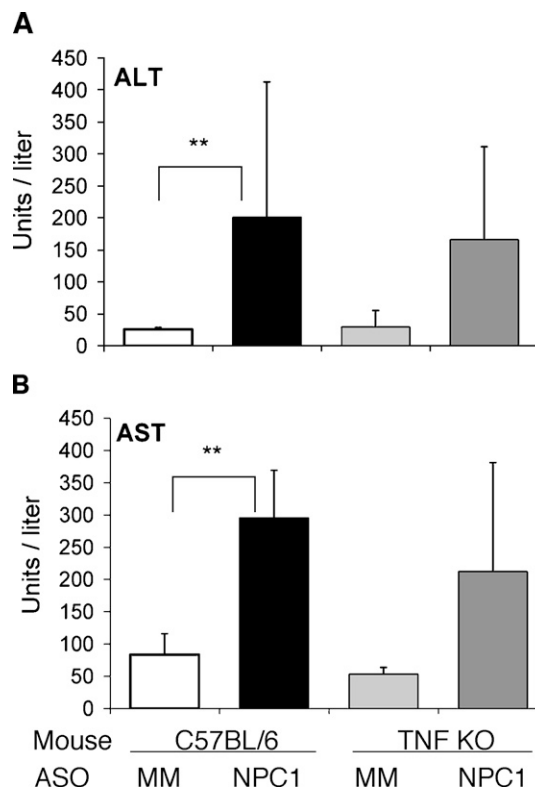


**Fig. 2.** Appearance of liver enzymes alanine aminotransferase (ALT) (A) and aspartate aminotransferase (AST) (B) in serum of C57BL/6 and TNF KO mice treated with mismatched (MM) and NPC1 ASOs. Each bar represents the mean  $\pm$  SD for 5–19 animals per treatment group. \*\* $P < 0.05$ .

inflammatory cells to lipogranulomas. This inflammatory cell recruitment was abolished in the absence of TNF- $\alpha$  (Fig. 5).

#### Knockout of TNF- $\alpha$ attenuates apoptosis and proliferation in NPC liver disease

Knockdown of NPC1 was previously shown to result in a 10-fold increase in the number of apoptotic hepatocytes, which was offset by proliferation of hepatic stellate cells (12). In this study, we found that 0.25% of cells were apoptotic in liver sections from C57BL/6 or TNF KO mice treated with mismatched ASO (Fig. 6A). The number of apoptotic cells was increased 5-fold by NPC1 knockdown. Remarkably, the lack of TNF- $\alpha$  resulted in a significant reduction in the number of apoptotic cells (Fig. 6A). These

TABLE 1. Unesterified cholesterol and sphingosine content of liver

Mouse	Unesterified Cholesterol		Sphingosine	
	MM ASO (n = 5)	NPC1 ASO (n = 5)	MM ASO (n = 3)	NPC1 ASO (n = 3)
	$\mu\text{g}/\mu\text{g protein}$		$\text{pmol}/\mu\text{g protein}$	
C57BL/6	0.007 $\pm$ 0.002	0.124 $\pm$ 0.014 <sup>a</sup>	47.6 $\pm$ 21.1	216.8 $\pm$ 26.5
TNF KO	0.011 $\pm$ 0.008	0.160 $\pm$ 0.040 <sup>b</sup>	93.0 $\pm$ 20.4	242.5 $\pm$ 77.5

MM, mismatched; ASO, antisense oligonucleotide. Values are means  $\pm$  SD.

<sup>a</sup> $P < 0.05$  (C57BL/6 MM ASO vs C57BL/6 NPC1 ASO).

<sup>b</sup> $P < 0.01$  (TNF KO MM ASO vs TNF KO NPC1 ASO).



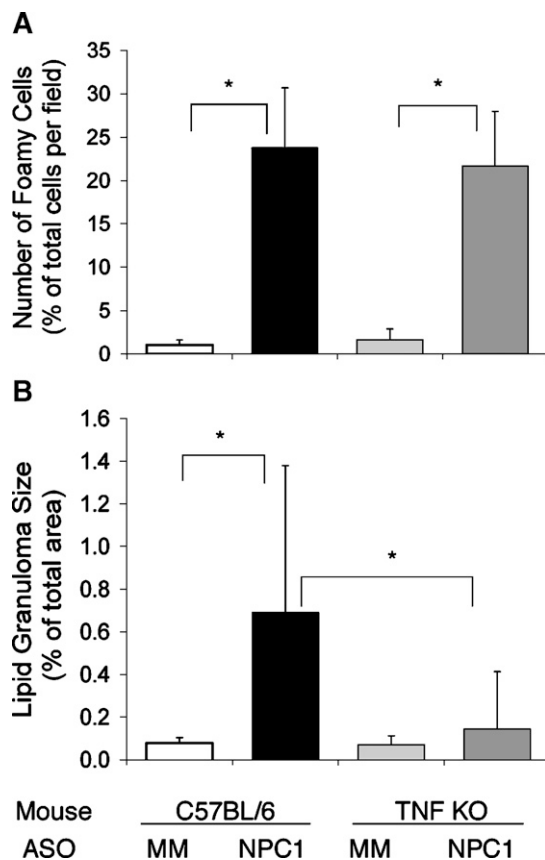


**Fig. 3.** Hepatic lipid accumulation in mismatched (MM) ASO and NPC1 ASO-treated C57BL/6 and TNF KO mice. **A:** Quantification of lipid-laden cells in which each bar represents the mean  $\pm$  SD from five animals in each treatment group. **B:** Quantification of lipid granuloma size in which each bar represents the mean  $\pm$  SD from five animals in each group. \* $P < 0.01$ .

data suggest that TNF- $\alpha$  signaling plays a role in hepatocyte apoptosis resulting from NPC1 dysfunction.

We previously determined that knockdown of NPC1 results in increased proliferation of hepatic stellate cells

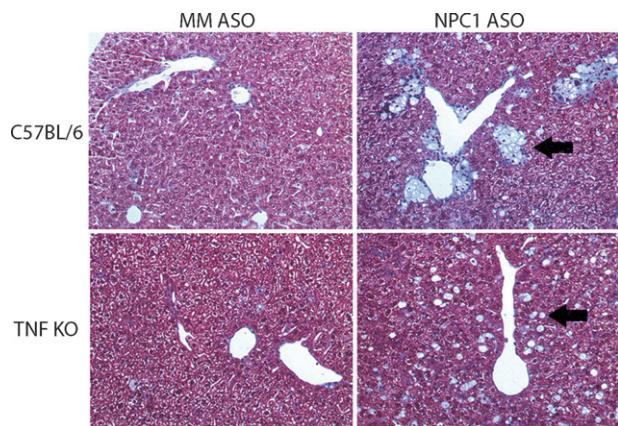


**Fig. 4.** Hepatic lipid accumulation and clustering of foamy macrophages in NPC1 knockdown mice. Masson's trichrome-stained liver sections from C57BL/6 and TNF KO mice treated with mismatched (MM) and NPC1 ASOs. Images at 200 $\times$  magnification. Black arrows indicate foamy macrophages.

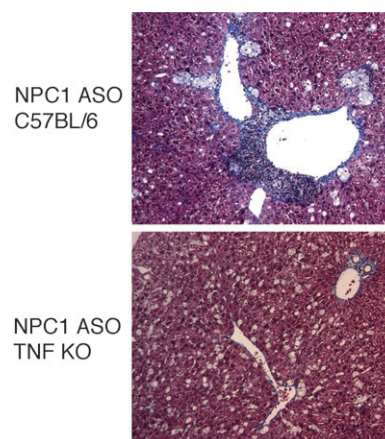


**Fig. 5.** Hepatic inflammation in mismatched and NPC1 ASO-treated C57BL/6 and TNF KO mice. Masson's trichrome-stained liver sections from NPC1 ASO-treated C57BL/6 and TNF KO mice. Images at 100 $\times$  magnification.

(12). To determine whether TNF- $\alpha$  plays a role in this process, we measured the number of BrdU-positive nuclei in liver tissue. In this study, we found knockdown of NPC1 in C57BL/6 mice resulted in 17-fold more proliferating cells compared with control. Lack of TNF- $\alpha$  resulted

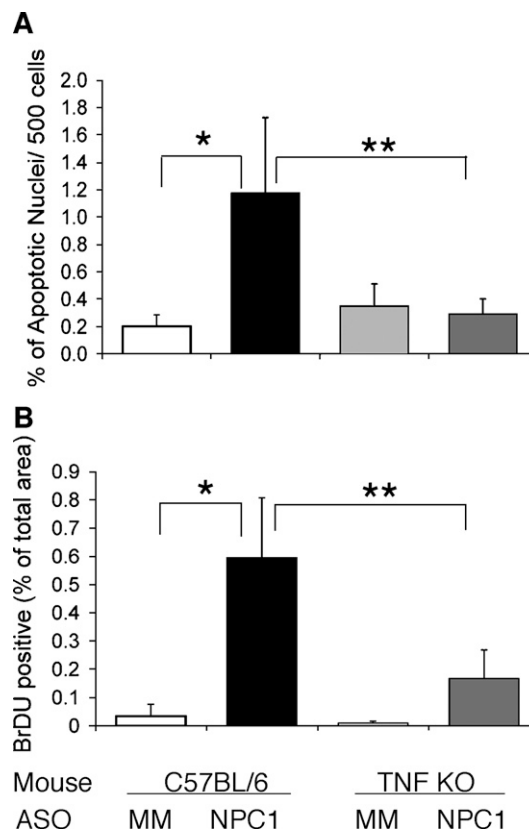


**Fig. 6.** NPC1 knockdown leads to fewer apoptotic and proliferative cells in the absence of TNF- $\alpha$ , but liver injury is unchanged. Quantification of apoptotic (A) and proliferating (B) cells in C7BL/6 and TNF KO mice treated with mismatched (MM) and NPC1 ASOs. Each bar represents the mean  $\pm$  SD for 5–19 animals per treatment group. \* $P < 0.01$ ; \*\* $P < 0.05$ .

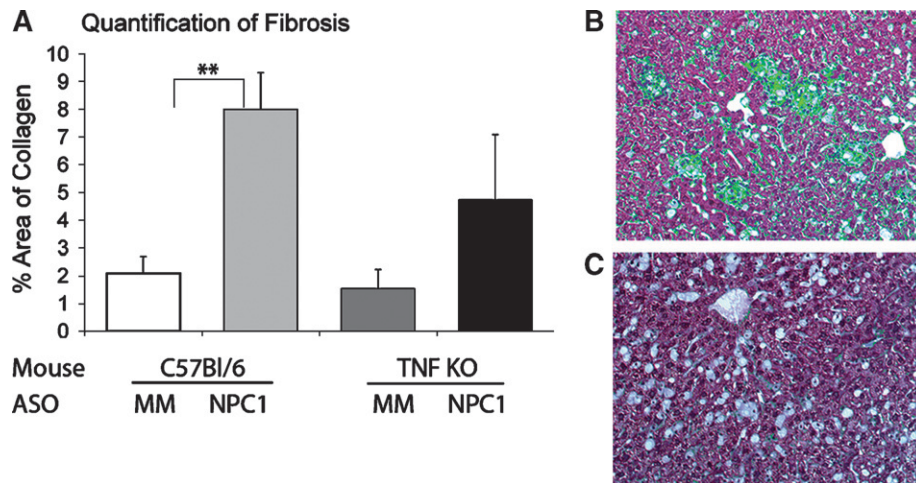


**Fig. 7.** NPC1 knockdown leads to less fibrosis in the absence of TNF- $\alpha$ . **A:** Quantification of collagen deposition in trichrome-stained liver sections from C57BL/6 and TNF KO mice treated with mismatched (MM) and NPC1 ASOs. The normal blue color of collagen has been replaced with green to allow quantification using the QuantiColor program. Representative images from NPC1 ASO-treated C57BL/6 (**B**) and TNF KO (**C**) liver sections reveal differences in collagen deposition. \*\*  $P < 0.05$ .

in a 3.5-fold reduction in the amount of proliferating cells (Fig. 6B).

#### Knockout of TNF- $\alpha$ results in decreased fibrosis and hepatic stellate cell activation

To determine the role of TNF- $\alpha$  in development of fibrosis, liver sections were stained with Masson's trichrome to visualize collagen deposition. Liver sections from C57BL/6 and TNF KO mice treated with mismatched ASOs showed

normal collagen staining around blood vessels, which is quantified in Fig. 6A. NPC1 knockdown in C57BL/6 mice led to a significant increase in the amount of collagen deposition (Fig. 7A), and most of the collagen surrounded clusters of foamy macrophages (Fig. 7B). Significant amounts of collagen were still deposited around blood vessels when NPC1 was knocked down in TNF KO mice; however, it was half that seen when NPC1 was knocked down in the presence of TNF- $\alpha$  (Fig. 7A, C). Given that there was reduced fibrosis,

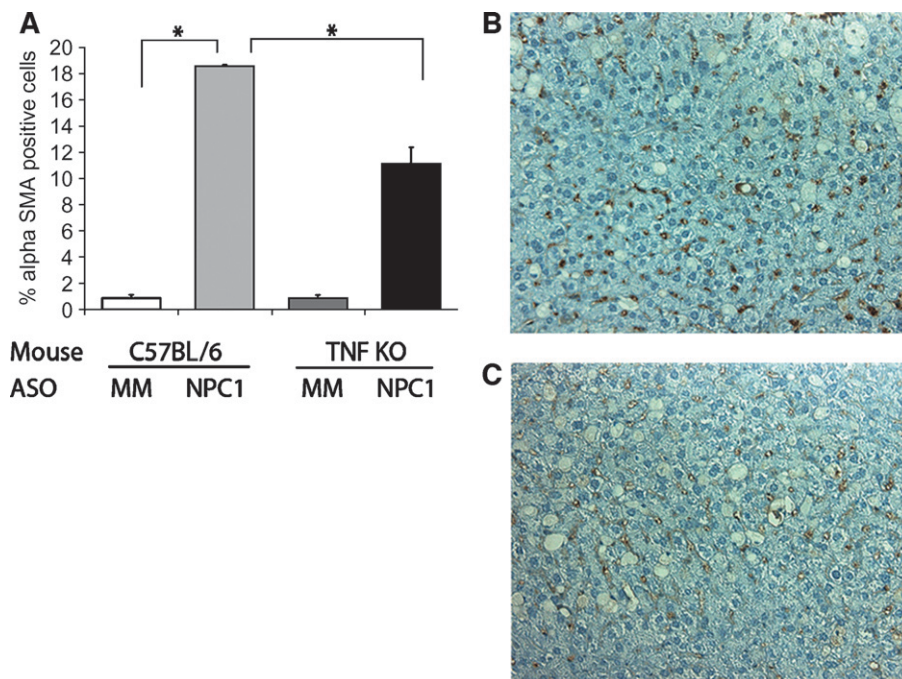


**Fig. 8.** NPC1 knockdown leads to less stellate cell activation in the absence of TNF- $\alpha$ . **A:** Quantification of immunohistochemistry for  $\alpha$ -smooth muscle actin was performed on liver sections from C57BL/6 (**B**) and TNF KO (**C**) mice treated with NPC1 ASOs. \*  $P < 0.01$ .

we hypothesize that fewer stellate cells were activated when NPC1 was knocked down in TNF KO mice.

To identify activated stellate cells, we performed  $\alpha$ -sma immunohistochemistry. Liver sections from mice treated with mismatched ASOs showed few stained cells (Fig. 8A), whereas NPC1 knockdown in C57BL/6 mice led to a 20-fold increase in the number of  $\alpha$ -sma-positive cells (Fig. 8A, B). NPC1 knockdown in TNF KO mice led to approximately 50% fewer  $\alpha$ -sma-positive cells (Fig. 8A, C).

## DISCUSSION

Our previous study showed that knockdown of NPC1 expression in mice leads to a disease phenotype that includes hepatomegaly, hepatic unesterified cholesterol storage, elevated liver enzymes, and hepatocyte apoptosis (12). The activation and proliferation of stellate cells produces collagen deposition and fibrosis. Foamy, vacuolated macrophages form and recruit inflammatory cell infiltrates. The goal of the current study was to identify the signals involved in the inflammatory process. TNF- $\alpha$  is an inflammatory cytokine that is released by injured hepatocytes. It activates stellate cells and Kupffer cells and recruits activated T cells. These cells secrete numerous cytokines and stimulate each other in a persistent inflammatory cycle that leads to liver fibrosis. Our hypothesis was that TNF- $\alpha$  plays a role in the progression of NPC liver disease because levels of TNF- $\alpha$  and its receptor, TNF-R1, are elevated in NPC mouse liver and brain (11–13). We tested this hypothesis by knocking down expression of NPC1 in control mice and mice lacking TNF- $\alpha$ .


Our results show that the presence or absence of TNF- $\alpha$  had no effect on the primary NPC phenotype of hepatomegaly and hepatic unesterified cholesterol storage; however, the physiological consequences of NPC cholesterol storage were blunted by the lack of TNF- $\alpha$ . There were significantly fewer apoptotic hepatocytes and proliferative stellate cells when NPC was knocked down in TNF- $\alpha$  knockout mice. Most striking was the effect on macrophages. NPC knockdown led to the formation of foamy, vacuolated macrophages in all mice, but the macrophages failed to cluster into large lipogranulomas in the absence of TNF- $\alpha$ .

The roles that Kupffer cells play in the initiation and propagation of hepatocyte apoptosis and fibrosis are poorly understood. Given that activated macrophages are important in NPC neuronal disease (26), their involvement in NPC liver disease may provide a common pathogenic thread. Future studies in which NPC1 is knocked down in macrophage-deficient mice may identify their involvement in hepatocyte apoptosis, inflammation, and fibrosis.

Our study also shows that TNF- $\alpha$  contributes to hepatocyte apoptosis in NPC liver disease. NPC1 knockdown leads to increased numbers of apoptotic hepatocytes when TNF- $\alpha$  is present but not when it is absent. Liver enzymes are identically increased in NPC1 ASO-treated mice independent of TNF- $\alpha$ . We attribute this to massive lipid accumulation due to NPC1 dysfunction. TNF KO animals

treated with NPC1 ASOs have cholesterol storage in their liver tissues identical to that in C57BL/6 mice treated with NPC1 ASOs. Previously, it has been shown that the amount of cholesterol taken up into the liver is directly correlated with the levels of liver injury in NPC<sup>nih</sup> mice (25).

The signals that link NPC1 dysfunction to TNF- $\alpha$  production are unknown. One possibility is that the lysosomal lipid accumulation damages lysosomal integrity and results in the release of lysosomal contents. There is precedent for lysosome disruption to lead to cell death (27–29). The lysosomal contents that would be released include cathepsins, cholesterol, and the products of sphingolipid digestion, e.g., ceramide, gangliosides, and sphingosine. In fact, sphingosine could be the lipid that initiates lysosome disruption. We and others (30, 31) have found that the level of sphingosine is significantly elevated in NPC liver. Cytosolic sphingosine is known to induce permeabilization of lysosomes, which initiates apoptosis (32). The elevated hepatic sphingosine that we observed could result from TNF- $\alpha$  binding to TNF-R1, which activates sphingomyelinase and ceramidase and generates sphingosine (33, 34). If this were the mechanism by which sphingosine accumulates in NPC disease, then we would expect to find hepatic sphingosine levels increased by NPC1 knockdown and the sphingosine increase to be less when TNF- $\alpha$  is absent; however, we find that hepatic sphingosine levels are increased to the same level by NPC1 knockdown in the presence or absence of TNF- $\alpha$ . This result suggests that the sphingosine is not downstream of TNF-R1 activation of sphingomyelinase. Instead, we attribute the increased sphingosine to lysosomal sequestration of the lipid and postulate that it may initiate lysosomal disruption and lead to hepatocyte injury. The damaged hepatocytes then initiate the inflammatory cycle by secreting TNF- $\alpha$ , which activates stellate and Kupffer cells and recruits activated T cells (20). As noted earlier, these activated cells secrete TNF- $\alpha$  and other cytokines, which escalates the inflammatory process.

There are no current therapies for NPC disease that delay onset of symptoms or prolong survival (35). An ideal treatment strategy would prevent or relieve the lipid storage and maintain normal liver and brain function. Our work shows that inflammation is a secondary consequence of lipid storage in NPC disease, and therefore, reducing inflammation would not be expected to lessen progression of the primary disease phenotype. Nevertheless, treatment with anti-inflammatory drugs may work synergistically with agents that reduce the lipid storage to prevent apoptosis, inflammation, and fibrosis. 

The authors thank Maribel Rios and Brigitte Huber at Tufts University for the use of their microscopes.

## REFERENCES

1. Vanier, M. T., and G. Millat. 2003. Niemann-Pick disease type C. *Clin. Genet.* **64**: 269–281.
2. Garver, W. S., G. A. Francis, D. Jelinek, G. Shepherd, J. Flynn, G. Castro, C. Walsh Vockley, D. L. Coppock, K. M. Pettit, R. A.



- Heidenreich, et al. 2007. The National Niemann-Pick C1 Disease Database: report of clinical features and health problems. *Am. J. Med. Genet. A*. **143A**: 1204–1211.
3. Reif, S., Z. Spirer, G. Messer, M. Baratz, B. Bembi, and Y. Bujanover. 1994. Severe failure to thrive and liver dysfunction as the main manifestations of a new variant of Niemann-Pick disease. *Clin. Pediatr. (Phila.)*. **33**: 628–630.
  4. Rutledge, J. C. 1989. Progressive neonatal liver failure due to type C Niemann-Pick disease. *Pediatr. Pathol.* **9**: 779–784.
  5. Putterman, C., J. Zelingher, and D. Shouval. 1992. Liver failure and the sea-blue histiocyte/adult Niemann-Pick disease. Case report and review of the literature. *J. Clin. Gastroenterol.* **15**: 146–149.
  6. Dumontel, C., C. Girod, F. Dijoud, Y. Dumez, and M. T. Vanier. 1993. Fetal Niemann-Pick disease type C: ultrastructural and lipid findings in liver and spleen. *Virchows Arch. A Pathol. Anat. Histopathol.* **422**: 253–259.
  7. Fu, L. S., T. C. Wu, C. R. Lai, and B. Huang. 1995. Niemann-Pick disease type C presenting as neonatal hepatitis: report of one case. *Zhonghua Min Guo Xiao Er Ke Yi Xue Hui Za Zhi*. **36**: 221–226.
  8. Zhou, H., R. P. Linke, H. E. Schaefer, W. Mobius, and U. Pfeifer. 1995. Progressive liver failure in a patient with adult Niemann-Pick disease associated with generalized AL amyloidosis. *Virchows Arch.* **426**: 635–639.
  9. Yerushalmi, B., R. J. Sokol, M. R. Narkewicz, D. Smith, J. W. Ashmead, and D. A. Wenger. 2002. Niemann-pick disease type C in neonatal cholestasis at a North American center. *J. Pediatr. Gastroenterol. Nutr.* **35**: 44–50.
  10. Kelly, D. A., B. Portmann, A. P. Mowat, S. Sherlock, and B. D. Lake. 1993. Niemann-Pick disease type C: diagnosis and outcome in children, with particular reference to liver disease. *J. Pediatr.* **123**: 242–247.
  11. Beltroy, E. P., J. A. Richardson, J. D. Horton, S. D. Turley, and J. M. Dietschy. 2005. Cholesterol accumulation and liver cell death in mice with Niemann-Pick type C disease. *Hepatology*. **42**: 886–893.
  12. Rimkunas, V. M., M. J. Graham, R. M. Crooke, and L. Liscum. 2008. In vivo antisense oligonucleotide reduction of NPC1 expression as a novel mouse model for Niemann Pick type C-associated liver disease. *Hepatology*. **47**: 1504–1512.
  13. Wu, Y. P., H. Mizukami, J. Matsuda, Y. Saito, R. L. Proia, and K. Suzuki. 2005. Apoptosis accompanied by up-regulation of TNF- $\alpha$  death pathway genes in the brain of Niemann-Pick type C disease. *Mol. Genet. Metab.* **84**: 9–17.
  14. Fausto, N., A. D. Laird, and E. M. Webber. 1995. Liver regeneration. 2. Role of growth factors and cytokines in hepatic regeneration. *FASEB J.* **9**: 1527–1536.
  15. Bradham, C. A., J. Plumpe, M. P. Manns, D. A. Brenner, and C. Trautwein. 1998. Mechanisms of hepatic toxicity. I. TNF-induced liver injury. *Am. J. Physiol.* **275**: G387–G392.
  16. Copaci, I., L. Micu, and M. Voiculescu. 2006. The role of cytokines in non-alcoholic steatohepatitis. A review. *J. Gastrointest. Liver Dis.* **15**: 363–373.
  17. Racanelli, V., and B. Rehmann. 2006. The liver as an immunological organ. *Hepatology*. **43 (Suppl)**: 54–62.
  18. Kolios, G., V. Valatas, and E. Kouroumalis. 2006. Role of Kupffer cells in the pathogenesis of liver disease. *World J. Gastroenterol.* **12**: 7413–7420.
  19. Bilzer, M., F. Roggel, and A. L. Gerbes. 2006. Role of Kupffer cells in host defense and liver disease. *Liver Int.* **26**: 1175–1186.
  20. Batailler, R., and D. A. Brenner. 2005. Liver fibrosis. *J. Clin. Invest.* **115**: 209–218.
  21. Crooke, R. M., M. J. Graham, K. M. Lemonidis, C. P. Whipple, S. Koo, and R. J. Perera. 2005. An apolipoprotein B antisense oligonucleotide lowers LDL cholesterol in hyperlipidemic mice without causing hepatic steatosis. *J. Lipid Res.* **46**: 872–884.
  22. Geary, R. S., T. A. Watanabe, L. Truong, S. Freier, E. A. Lesnik, N. B. Sioufi, H. Sasmor, M. Manoharan, and A. A. Levin. 2001. Pharmacokinetic properties of 2'-O-(2-methoxyethyl)-modified oligonucleotide analogs in rats. *J. Pharmacol. Exp. Ther.* **296**: 890–897.
  23. Folch, J., M. Lees, and G. H. Sloane Stanley. 1957. A simple method for the isolation and purification of total lipides from animal tissues. *J. Biol. Chem.* **226**: 497–509.
  24. Bielawski, J., Z. M. Szulc, Y. A. Hannun, and A. Bielawska. 2006. Simultaneous quantitative analysis of bioactive sphingolipids by high-performance liquid chromatography-tandem mass spectrometry. *Methods*. **39**: 82–91.
  25. Beltroy, E. P., B. Liu, J. M. Dietschy, and S. D. Turley. 2007. Lysosomal unesterified cholesterol content correlates with liver cell death in murine Niemann-Pick type C disease. *J. Lipid Res.* **48**: 869–881.
  26. Repa, J. J., H. Li, T. C. Frank-Cannon, M. A. Valasek, S. D. Turley, M. G. Tansey, and J. M. Dietschy. 2007. Liver X receptor activation enhances cholesterol loss from the brain, decreases neuroinflammation, and increases survival of the NPC1 mouse. *J. Neurosci.* **27**: 14470–14480.
  27. Bursch, W. 2001. The autophagosomal-lysosomal compartment in programmed cell death. *Cell Death Differ.* **8**: 569–581.
  28. Boya, P., K. Andreau, D. Poncet, N. Zamzami, J. L. Perfettini, D. Metivier, D. M. Ojcius, M. Jaattela, and G. Kroemer. 2003. Lysosomal membrane permeabilization induces cell death in a mitochondrion-dependent fashion. *J. Exp. Med.* **197**: 1323–1334.
  29. Guicciardi, M. E., M. Leist, and G. J. Gores. 2004. Lysosomes in cell death. *Oncogene*. **23**: 2881–2890.
  30. Goldin, E., C. F. Roff, S. P. Miller, C. Rodriguez-Lafrasse, M. T. Vanier, R. O. Brady, and P. G. Pentchev. 1992. Type C Niemann-Pick disease: a murine model of the lysosomal cholesterol lipidosis accumulates sphingosine and sphinganine in liver. *Biochim. Biophys. Acta*. **1127**: 303–311.
  31. Roff, C. F., E. Goldin, M. E. Comly, J. Blanchette-Mackie, A. Cooney, R. O. Brady, and P. G. Pentchev. 1992. Niemann-Pick type-C disease: deficient intracellular transport of exogenously derived cholesterol. *Am. J. Med. Genet.* **42**: 593–598.
  32. Chwieralski, C. E., T. Welte, and F. Buhling. 2006. Cathepsin-regulated apoptosis. *Apoptosis*. **11**: 143–149.
  33. Kuno, K., K. Sukegawa, Y. Ishikawa, T. Orii, and K. Matsushima. 1994. Acid sphingomyelinase is not essential for the IL-1 and tumor necrosis factor receptor signaling pathway leading to NF $\kappa$ B activation. *Int. Immunol.* **6**: 1269–1272.
  34. Mari, M., and J. C. Fernandez-Checa. 2007. Sphingolipid signalling and liver diseases. *Liver Int.* **27**: 440–450.
  35. Patterson, M. C., and F. Platt. 2004. Therapy of Niemann-Pick disease, type C. *Biochim. Biophys. Acta*. **1685**: 77–82.